

Seismic critical-angle reflectometry: A method to characterize azimuthal anisotropy?

Martin Landrø¹ and Ilya Tsvankin²

ABSTRACT

Existing anisotropic parameter-estimation algorithms that operate with long-offset data are based on the inversion of either nonhyperbolic moveout or wide-angle amplitude-variation-with-offset (AVO) response. We show that valuable information about anisotropic reservoirs can also be obtained from the critical angle of reflected waves. To explain the behavior of the critical angle, we develop weak-anisotropy approximations for vertical transverse isotropy and then use Tsvankin's notation to extend them to azimuthally anisotropic models of orthorhombic symmetry. The P-wave critical-angle reflection in orthorhombic media is particularly sensitive to the parameters $\epsilon^{(1)}$ and $\epsilon^{(2)}$ responsible for the symmetry-plane horizontal velocity in the high-velocity layer. The azimuthal variation of the critical angle for typical orthorhombic models can reach 5° – 6° , which translates into substantial changes in the critical offset of the reflected P-wave. The main diagnostic features of the critical-angle reflection employed in our method include the rapid amplitude increase at the critical angle and the subsequent separation of the head wave. Analysis of exact synthetic seismograms, generated with the reflectivity method, confirms that the azimuthal variation of the critical offset is detectable on wide-azimuth, long-spread data and can be qualitatively described by our linearized equations. Estimation of the critical offset from the amplitude curve of the reflected wave, however, is not straightforward. Additional complications may be caused by the overburden noise train and by the influence of errors in the overburden velocity model on the computation of the critical angle. Still, critical-angle reflectometry should help to constrain the dominant fracture directions and can be combined with other methods to reduce the uncertainty in the estimated anisotropy parameters.

INTRODUCTION

It is now widely accepted in the petroleum industry that most subsurface formations are anisotropic with respect to seismic wave propagation. Estimation of the anisotropy parameters required to build reliable velocity models, however, remains a challenging and often ill-posed problem (e.g., Tsvankin, 2005; Tsvankin and Grechka, 2006).

Long-offset reflection data play an important role in anisotropic velocity analysis because they are recorded for a wide range of angles with the vertical. In particular, inversion of P-wave nonhyperbolic (long-spread) moveout for transversely isotropic media with a vertical symmetry axis (VTI) is often used to estimate the anellipticity parameter η , which controls time processing of P-wave data (Alkhalifah and Tsvankin, 1995; Alkhalifah, 1997; Toldi et al., 1999). Nonhyperbolic moveout analysis has also been extended to more complicated, azimuthally anisotropic media composed of orthorhombic layers (Pech and Tsvankin, 2004; Vasconcelos and Tsvankin, 2006). Despite a number of generally successful case studies (e.g., Toldi et al., 1999), nonhyperbolic moveout inversion is hampered by the trade-off between the normal-moveout (NMO) velocity and the quartic moveout coefficient. Even relatively low levels of correlated noise can create substantial uncertainty in the estimation of the parameter η in VTI media or the corresponding anellipticity parameters of orthorhombic media (Grechka and Tsvankin, 1998, 1999). On the whole, while nonhyperbolic moveout inversion helps in time processing of reflection data, its application in reservoir characterization is much more problematic.

Another shortcoming of travelttime-inversion methods is their low vertical resolution, especially for relatively deep reservoirs. Higher resolution can be achieved by amplitude-variation-with-offset (AVO) analysis, which provides information about the local elastic properties at the reservoir level. In particular, the azimuthal variation of the AVO response measured over fractured reservoirs is often used to estimate the fracture orientation and identify areas of intense fracturing (Rüger, 2001; Gray et al., 2002; Hall and Kendall, 2003).

Manuscript received by the Editor July 18, 2006; revised manuscript received December 12, 2006; published online March 19, 2007.

¹Norwegian University of Science and Technology, Department of Petroleum Engineering and Applied Geophysics, Trondheim, Norway. E-mail: martin.landro@ntnu.no.

²Colorado School of Mines, Center for Wave Phenomena, Department of Geophysics, Golden, Colorado. E-mail: ilya@mines.edu.

© 2007 Society of Exploration Geophysicists. All rights reserved.

Most existing AVO algorithms operate with the AVO gradient estimated from conventional-spread reflection data. Although including longer offsets significantly reduces the ambiguity of the amplitude inversion, especially for multicomponent data (Jilek, 2002), wide-angle AVO analysis is not yet common (Pankhurst et al., 2002). Even when the offset-to-depth ratio is sufficient to constrain the large-angle AVO terms, the low data quality and phase changes at long offsets cause serious complications for accurate amplitude picking.

Here, we suggest another way of employing long-offset data in anisotropic parameter estimation. When the P-wave velocity in a hydrocarbon reservoir is higher than that in the cap rock, it may be possible to record critical and post-critical reflections from the top of the reservoir layer. For low-velocity reservoirs, critical reflections are generated at the bottom of the reservoir. Landrø et al. (2004) proposed to measure the shift in the critical angle or offset observed on time-lapse data to monitor reservoir production. If either the cap or reservoir layer is azimuthally anisotropic, the critical angle and the corresponding critical offset vary with azimuth. For 3D data with good coverage in azimuth and offset, the azimuthal variation of the critical angle can be used to identify the vertical symmetry planes of the model and constrain the anisotropy parameters. In contrast to AVO analysis, this method does not require accurate amplitude measurements for a wide range of offsets because the critical angle can be estimated from the point of the fastest increase of the reflection amplitude.

We begin by briefly introducing ultrasonic critical-angle reflectometry based on laboratory measurements of the critical angle in various materials. Then we derive a concise weak-anisotropy approximation for the critical angle in VTI media and generalize this result for orthorhombic models used to describe naturally fractured reservoirs. The analytic results help to identify the parameter combinations constrained by critical-angle measurements. To evaluate the feasibility of estimating the critical angle for orthorhombic media, we compute full-waveform, synthetic seismograms using the reflectivity method. Finally, we discuss practical issues related to field-data application of the method.

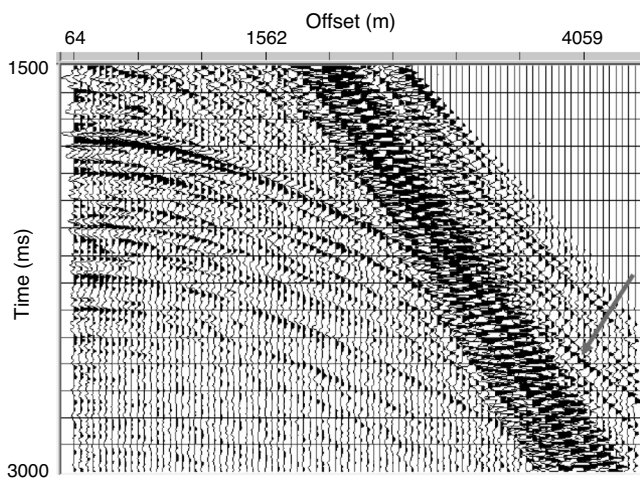


Figure 1. Common-receiver field gather of the vertical displacement component. The arrow marks a reflection from the top of a high-velocity layer.

ULTRASONIC AND SEISMIC CRITICAL-ANGLE REFLECTOMETRY

This paper extends to seismology the idea of the well-established method of ultrasonic measurements called *ultrasonic critical-angle reflectometry*. The method is based on measuring the critical angle as a function of azimuth in human bones, some composite materials, etc. (Antich and Mehta, 1997). The shift of the critical angle with azimuth is then inverted for the pertinent anisotropy parameters. Ultrasonic critical-angle reflectometry has become the industry standard for a wide range of applications.

Although postcritical reflections are well documented in seismological literature, implementation of quantitative critical-angle reflectometry is not straightforward. First, target horizons (reservoirs) are often located at significant depths and overlaid by a complex sequence of sedimentary layers. Multiple reflections and mode conversions in the overburden can create interference with the critical-angle event from the reservoir. Second, the method requires a substantial velocity increase at the top or bottom of the target layer, which is not always the case for hydrocarbon reservoirs. Third, wide-azimuth, long-offset data, which are needed to reconstruct the azimuthal variation of the critical angle, are routinely acquired only in ocean bottom cable (OBC) multicomponent surveys. Marine streamer data sets typically have narrow azimuthal coverage, while full-azimuth land data seldom include sufficiently long offsets.

Still, under favorable circumstances the critical angle can be detected on seismic reflection data. Figure 1 displays a raw seismic gather that contains an interpretable reflection from a boundary with a large positive velocity contrast. Despite the interference with noise and overburden events, this reflection can be identified for large offsets up to about 4.5 km. The interfering arrivals were attenuated by standard $f-k$ filtering (Figure 2). To make noise suppression near the critical angle more effective, the filtering was applied with a narrow range of apparent velocities, which attenuated the target event at near offsets.

Then, amplitude analysis (Figure 3) was used to identify the point of the fastest amplitude increase (the inflection point), which is supposed to correspond to the critical offset x_{cr} . The value of $x_{cr} \approx 4$ km estimated from the AVO curve is in good agreement with an independent prediction made using borehole data (well logs) from the area. This case study supports the feasibility of critical-angle reflectometry in the presence of a significant velocity contrast at the target level.

CRITICAL ANGLE FOR VTI AND ORTHORHOMBIC MEDIA

We consider a plane P- or S-wave incident upon a horizontal interface that separates two anisotropic media. If the transmitted wave (again, it can be P or S) has a higher velocity, for a certain incidence angle its group-velocity vector becomes horizontal. This angle, which is usually called critical, depends on the phase-velocity function and, therefore, is influenced by the velocity anisotropy. For simplicity, we assume that the reflector coincides with a symmetry plane in the reflecting medium, which implies that the phase-velocity vector of the transmitted wave at the critical angle is also horizontal. Ac-

cording to Snell's law, the horizontal slowness component of all reflected and transmitted waves should be equal to that of the incident wave, which yields

$$\frac{\sin \theta_{cr}}{V_1(\theta_{cr})} = \frac{1}{V_{hor,2}}, \quad (1)$$

where θ_{cr} is the critical phase angle with the vertical, $V_1(\theta)$ is the phase velocity in the incidence medium, and $V_{hor,2}$ is the horizontal phase velocity in the reflecting medium. The subscripts 1 and 2 denote the incident and reflecting media, respectively. All quantities in equation 1 are computed in the vertical plane that contains the slowness vector of the incident wave. Note that the corresponding critical ray may not lie in the same vertical plane if the wave propagates outside symmetry planes in azimuthally anisotropic media.

The critical angle for a particular wave mode (e.g., PP, SS, or SP) can be found by solving equation 1 with the appropriate phase-velocity function $V_1(\theta)$ and the horizontal velocity $V_{hor,2}$. An alternative way of computing the critical angle, often used in deriving reflection and transmission coefficients, is based on expressing the Christoffel equation (e.g., Helbig, 1994) in the incidence medium in terms of the slowness components and solving it for the horizontal slowness equal to $1/V_{hor,2}$. For point-source radiation, the segment of the wavefront orthogonal to the critical phase direction θ_{cr} is responsible for generating the head wave, which interferes with the reflected wave in the post-critical domain.

VTI media

For transversely isotropic models with a vertical symmetry axis (VTI), the velocity function and the critical angle are azimuthally invariant. The P-wave horizontal velocity in VTI media is expressed through the vertical velocity V_{p0} and Thomsen parameter ϵ as

$$V_{hor} = V_{p0} \sqrt{1 + 2\epsilon}. \quad (2)$$

If the incidence medium is isotropic with the velocity $V_{p0,1}$, the exact P-wave critical angle from equation 1 is given by

$$\sin \theta_{cr} = \frac{V_{p0,1}}{V_{p0,2} \sqrt{1 + 2\epsilon_2}}. \quad (3)$$

To express the critical angle for a VTI/VTI interface as a simple function of the anisotropy parameters, we employ the weak-anisotropy approximation for the phase-velocity function in the incidence medium (Thomsen, 1986):

$$V_1(\theta) = V_{p0,1} (1 + \delta_1 \sin^2 \theta \cos^2 \theta + \epsilon_1 \sin^4 \theta). \quad (4)$$

Equation 4 is linearized in the parameters ϵ_1 and δ_1 . Similarly, the horizontal velocity in the reflecting medium can be linearized in ϵ_2 :

$$V_{hor,2} = V_{p0,2} (1 + \epsilon_2). \quad (5)$$

Assuming $V_{p0,2} > V_{p0,1}$ and substituting equations 4 and 5 into equation 1, we find

$$\sin \theta_{cr} = \frac{V_{p0,1} (1 + \delta_1 \sin^2 \theta_{cr} \cos^2 \theta_{cr} + \epsilon_1 \sin^4 \theta_{cr})}{V_{p0,2} (1 + \epsilon_2)}. \quad (6)$$

Within the framework of the linearized approximation, the angle θ_{cr} , in the terms involving ϵ and δ , can be replaced by its isotropic value $\theta_{cr,is}$:

$$\sin \theta_{cr,is} = \frac{V_{p0,1}}{V_{p0,2}} = n; \quad (7)$$

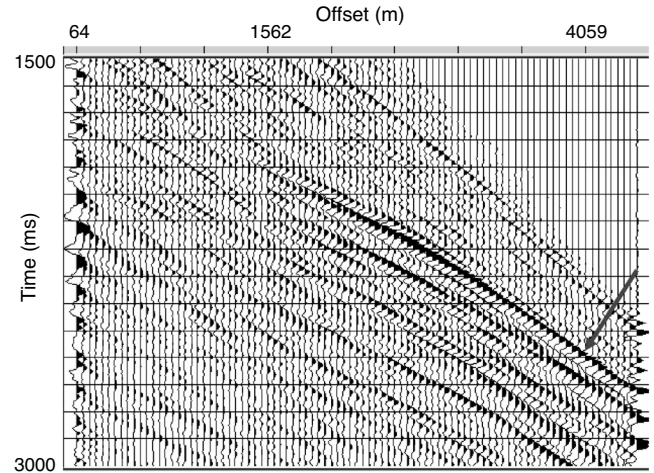


Figure 2. Gather from Figure 1 after application of f - k filtering designed to attenuate the overburden noise. The target event marked in Figure 1 is clearly visible at offsets larger than 1500 m.

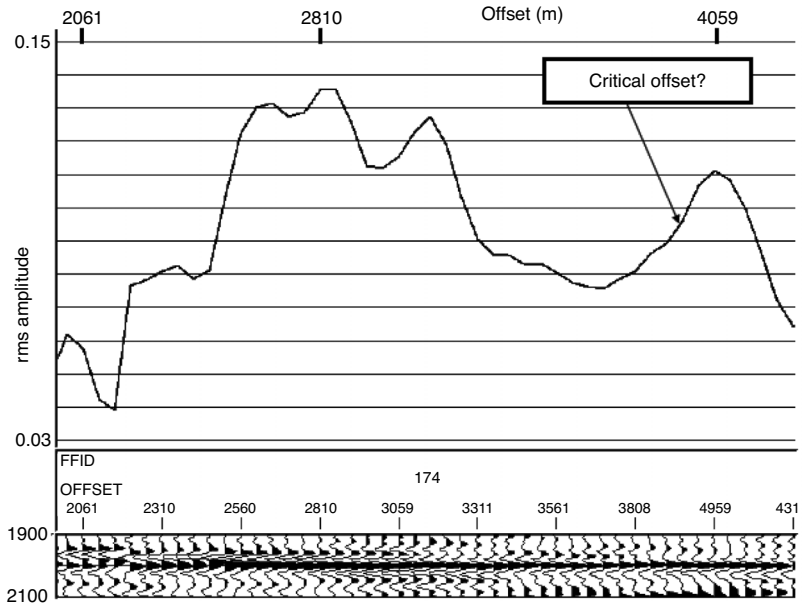


Figure 3. Estimated rms amplitude of the target event from Figures 1 and 2 computed in a 50 ms window after f - k filtering. The offset of the fastest amplitude increase, which we interpret as corresponding to the critical-angle reflection, is near the 4-km mark. The windowed section on the bottom shows the flattened target event.

the velocity ratio n is sometimes called the *refraction index*. Then the right-hand side of equation 6 no longer contains the unknown critical angle:

$$\sin \theta_{cr} = \frac{V_{P0,1} [1 + \delta_1 n^2 (1 - n^2) + \epsilon_1 n^4]}{V_{P0,2} (1 + \epsilon_2)}. \quad (8)$$

After further linearization in ϵ_2 , we find

$$\sin \theta_{cr} = n [1 - \epsilon_2 + \delta_1 n^2 + (\epsilon_1 - \delta_1) n^4]. \quad (9)$$

Because the vertical-velocity ratio $n < 1$, the critical angle is particularly sensitive to the parameter ϵ_2 responsible for the P-wave horizontal velocity in the reflecting medium.

If the incidence medium is anisotropic, the critical offset is determined by the critical group (ray) angle ψ_{cr} , which can be computed from θ_{cr} using the well-known group-velocity equations for VTI media. In the weak-anisotropy approximation (Tsvankin, 2005),

$$\psi_{cr} = \theta_{cr} + [\delta_1 + 2(\epsilon_1 - \delta_1) \sin^2 \theta_{cr}] \sin 2\theta_{cr}. \quad (10)$$

Orthorhombic media

Many naturally fractured reservoirs are believed to possess orthorhombic symmetry in the long-wavelength limit (Bakulin et al., 2000; Grechka and Kachanov, 2006). Note that most existing parameter-estimation methods for orthorhombic models rely on multicomponent data (e.g., Grechka et al., 2005), which are not acquired in the bulk of seismic surveys.

Suppose a horizontal interface separates two orthorhombic media with the same orientation of the symmetry planes (there are three mutually orthogonal symmetry planes in orthorhombic models). One of the symmetry planes is assumed to coincide with the horizontal reflector, so the critically refracted ray corresponds to a horizontal

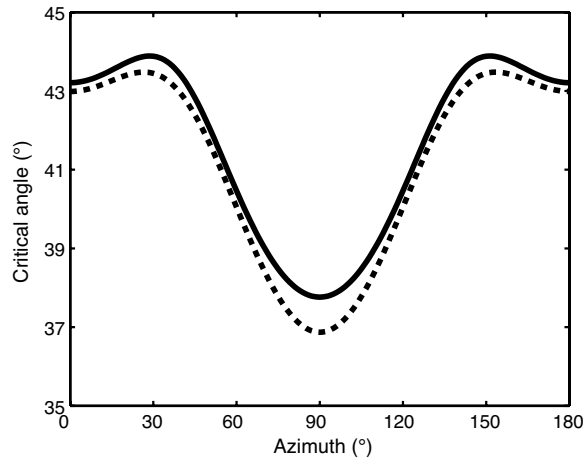


Figure 4. Critical angle of P-waves as a function of azimuth for an interface between isotropic (incidence) and orthorhombic (reflecting) media. The azimuth ϕ is measured from the symmetry plane $[x_1, x_3]$. The solid curve is the exact angle θ_{cr} computed from equation 1 using the phase-velocity function given in Tsvankin (1997); the dashed curve is the weak-anisotropy approximation 15. The P-wave velocity in the isotropic medium is $V_{P0,1} = 2100$ m/s; the relevant parameters of the orthorhombic medium are $V_{P0,2} = 2800$ m/s, $\epsilon_2^{(1)} = 0.25$, $\epsilon_2^{(2)} = 0.1$, and $\delta_2^{(3)} = -0.1$. The azimuthal anisotropy beneath the reflector causes a noticeable variation of the critical angle with azimuth.

slowness vector. For convenience, the vertical symmetry planes in both media are aligned with the coordinate planes $[x_1, x_3]$ and $[x_2, x_3]$.

All kinematic VTI equations can be easily adapted for the vertical symmetry planes using the anisotropy parameters introduced in Tsvankin (1997, 2005). For example, if the incidence medium is isotropic, the exact critical angle in the $[x_1, x_3]$ -plane is obtained from equation 3:

$$\sin \theta_{cr} (\phi = 0^\circ) = \frac{V_{P0,1}}{V_{P0,2} \sqrt{1 + 2\epsilon_2^{(2)}}}, \quad (11)$$

where ϕ is the azimuth from the x_1 -axis, and the parameter $\epsilon_2^{(2)}$ is defined in the $[x_1, x_3]$ -plane by analogy with the VTI parameter ϵ (the superscript 2 refers to the x_2 -axis orthogonal to the $[x_1, x_3]$ -plane).

When both media are orthorhombic, the weak-anisotropy approximation for the critical angle in the $[x_1, x_3]$ -plane can be found from equation 9:

$$\sin \theta_{cr} (\phi = 0^\circ) = n [1 - \epsilon_2^{(2)} + \delta_1^{(2)} n^2 + (\epsilon_1^{(2)} - \delta_1^{(2)}) n^4]; \quad (12)$$

the parameter $\delta^{(2)}$ is defined in the $[x_1, x_3]$ -plane by analogy with δ . Replacing the parameters $\epsilon^{(2)}$ and $\delta^{(2)}$ in equations 11 and 12 by $\epsilon^{(1)}$ and $\delta^{(1)}$, respectively, yields the critical angles in the $[x_2, x_3]$ -plane.

In the weak-anisotropy limit, the kinematic analogy between orthorhombic and VTI media remains valid for 2D P-wave propagation even outside the symmetry planes, if the parameters ϵ and δ are expressed as the following functions of azimuth (Tsvankin, 1997, 2005):

$$\delta(\phi) = \delta^{(1)} \sin^2 \phi + \delta^{(2)} \cos^2 \phi, \quad (13)$$

$$\begin{aligned} \epsilon(\phi) = & \epsilon^{(1)} \sin^4 \phi + \epsilon^{(2)} \cos^4 \phi + (2\epsilon^{(2)} \\ & + \delta^{(3)}) \sin^2 \phi \cos^2 \phi; \end{aligned} \quad (14)$$

the parameter $\delta^{(3)}$ is defined in the horizontal plane. Substituting $\delta(\phi)$ and $\epsilon(\phi)$ from equations 13 and 14 into equation 9, we obtain the linearized P-wave critical angle for an arbitrary azimuth ϕ :

$$\sin \theta_{cr}(\phi) = n \{ 1 - \epsilon_2(\phi) + \delta_1(\phi) n^2 + [\epsilon_1(\phi) - \delta_1(\phi)] n^4 \}. \quad (15)$$

As was the case for VTI media, if the incidence medium is anisotropic, the critical offset is determined by the group angle that corresponds to the critical phase angle θ_{cr} .

Numerical examples

The magnitude of the azimuthal variation of the critical angle for typical orthorhombic models (e.g., Bakulin et al., 2000; Tsvankin, 2005) and the accuracy of the weak-anisotropy approximation are illustrated in Figures 4-6. When the incidence medium is isotropic, the dependence of θ_{cr} on the azimuth ϕ is controlled by the P-wave velocity in the horizontal plane of the reflecting orthorhombic medium (equation 1). In the weak-anisotropy approximation, the horizontal velocity in the reflecting medium is described by the parameter $\epsilon_2(\phi)$ (equations 14 and 15).

The difference between the horizontal velocities in the symmetry planes is approximately proportional to $\epsilon_2^{(1)} - \epsilon_2^{(2)}$. For the model in Figure 4, $\epsilon_2^{(1)} - \epsilon_2^{(2)} = 0.15$, which translates into a change in θ_{cr} between the symmetry planes that exceeds 5° . The extrema of the function $\theta_{cr}(\phi)$, however, do not necessarily coincide with the symmetry-

plane directions. The maximum of θ_{cr} at an azimuth close to 30° in Figure 4 is associated with a decrease in the P-wave horizontal velocity away from the $[x_1, x_3]$ -plane caused by the negative value of $\delta_2^{(3)}$ (Tsvankin, 2005). After reaching a minimum at $\phi \approx 30^\circ$, the velocity increases toward the symmetry plane $[x_2, x_3]$, which reduces the critical angle for azimuths $\phi > 30^\circ$.

The model in Figure 5 has a smaller value (0.05) of the difference $\epsilon_2^{(1)} - \epsilon_2^{(2)}$, and the maximum azimuthal variation of the critical angle is limited to about 3° . A significant part of this variation is related to the increase in θ_{cr} with azimuth away from the $[x_1, x_3]$ -plane. For both models, the weak-anisotropy approximation does not deviate far from the exact solution and correctly reproduces the trend of $\theta_{cr}(\phi)$.

When the incidence medium is orthorhombic (Figure 6), the critical angle becomes a function of all five anisotropy parameters responsible for the P-wave velocity above the reflector ($\epsilon_1^{(1)}, \epsilon_1^{(2)}, \delta_1^{(1)}, \delta_1^{(2)}$, and $\delta_1^{(3)}$). If the reflecting medium is isotropic, the azimuthal variation of θ_{cr} replicates that of the phase velocity at the critical angle. As was the case in Figures 4 and 5, the azimuthal dependence of the critical angle in Figure 6 is more pronounced for the model with a larger difference between the ϵ -parameters defined in the vertical symmetry planes (this time, it is $\epsilon_1^{(1)}$ and $\epsilon_1^{(2)}$).

Variations in the critical angle on the order of 5° – 6° would change the critical offset for deep interfaces by hundreds of meters, which should be detectable on AVO plots similar to the one in Figure 3. Application of our method requires acquisition of long-offset, wide-azimuth data with a sufficiently high signal-to-noise ratio at near-critical offsets. Since the function $\theta_{cr}(\phi)$ may have extrema between the symmetry planes, dense azimuthal coverage may be essential for the success of critical-angle reflectometry.

Critical angles for mode-converted and S-waves

Analysis of PS- and SS-waves here is restricted to VTI media and symmetry planes of orthorhombic models. Analytic description of S-waves outside symmetry planes of azimuthally anisotropic media is much more complicated and cannot be based on the analogy with vertical transverse isotropy. Equation 9 can be adapted for mode-converted and S-waves in VTI media by applying the substitution rule described in Tsvankin (2005). In the weak-anisotropy limit, any kinematic signature of SV-waves can be obtained from the corresponding P-wave approximation by replacing V_{p0} with the S-wave vertical velocity V_{s0} , δ with the SV-wave velocity parameter $\sigma \equiv (V_{p0}/V_{s0}^2)(\epsilon - \delta)$, and setting ϵ in the P-wave equation to zero.

Using this recipe, the critical angle for the SS (i.e., SVSV) transmission into the high-velocity medium can be found from equation 9 as

$$\sin \theta_{cr,SS} = n_{SS} [1 + \sigma_1 n_{SS}^2 - \sigma_1 n_{SS}^4], \quad (16)$$

where $n_{SS} \equiv V_{s0,1}/V_{s0,2}$.

Similarly, for the S-to-P (i.e., SV-to-P) transmission we have:

$$\sin \theta_{cr,SP2} = n_{SP2} [1 - \epsilon_2 + \sigma_1 n_{SP2}^2 - \sigma_1 n_{SP2}^4]; \quad (17)$$

$n_{SP2} \equiv V_{s0,1}/V_{p0,2}$

For the S-to-P reflection in the incidence medium,

$$\sin \theta_{cr,SP1} = n_{SP1} [1 - \epsilon_1 + \sigma_1 n_{SP1}^2 - \sigma_1 n_{SP1}^4]; \quad (18)$$

$n_{SP1} \equiv V_{s0,1}/V_{p0,1}$.

Equations 16–18 remain valid for SV-waves in the vertical symmetry planes of orthorhombic media. The critical angles of pure

S-waves and converted waves can be identified from the corresponding amplitude anomalies of the reflected SS-wave. Note that the accuracy of the weak-anisotropy approximation for SV-waves usually is much lower than for P-waves because of the relatively large values of the parameter σ (Tsvankin, 2005).

In the untypical case of an extremely strong velocity contrast, the SV-wave velocity in the reflecting layer ($V_{s0,2}$) can be higher than the P-wave velocity in the incidence medium ($V_{p0,1}$). Then application of the substitution rule yields the following critical angle for the P-to-S transmission:

$$\sin \theta_{cr,PS} = n_{PS} [1 + \delta_1 n_{PS}^2 + (\epsilon_1 - \delta_1) n_{PS}^4]; \quad (19)$$

$n_{PS} \equiv V_{p0,1}/V_{s0,2}$. If the vertical-velocity ratio is known, the critical angle of PS-waves provides a relationship between the parameters ϵ_1 and δ_1 .

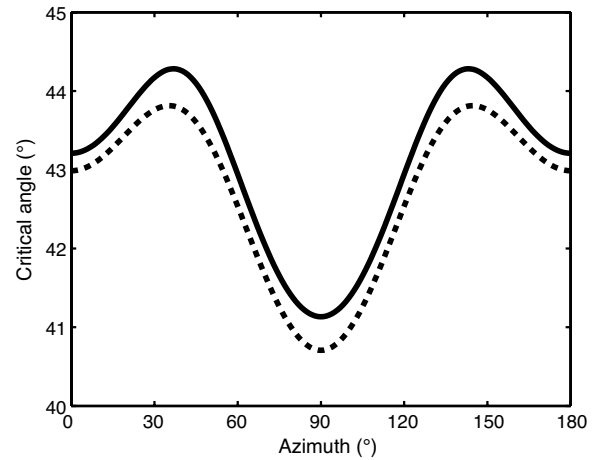


Figure 5. Critical angle of P-waves for an interface between isotropic (incidence) and orthorhombic (reflecting) media. The model parameters are the same as those in Figure 4, except for $\epsilon_2^{(1)} = 0.15$.

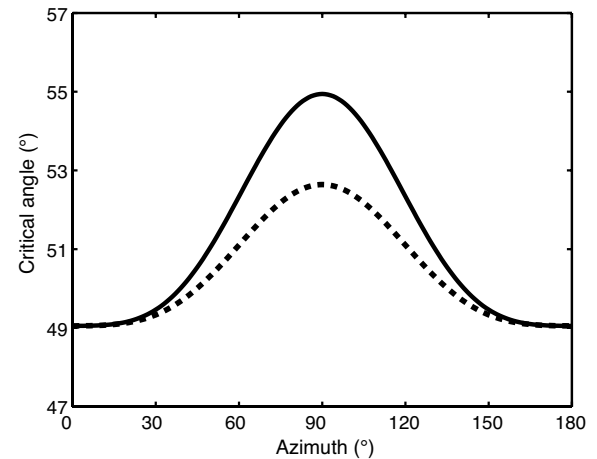


Figure 6. Critical angle of P-waves obtained from the weak-anisotropy approximation 15 for an interface between orthorhombic (incidence) and isotropic (reflecting) media. The solid curve is computed for the following parameters of the orthorhombic medium: $V_{p0,1} = 2100$ m/s, $\epsilon_1^{(1)} = 0.25$, $\epsilon_1^{(2)} = 0.1$, $\delta_1^{(1)} = 0.05$, $\delta_1^{(2)} = -0.1$, and $\delta_1^{(3)} = -0.1$. For the dashed curve, all parameters are the same, except for $\epsilon_1^{(1)} = 0.15$. The P-wave velocity in the isotropic medium is $V_{p0,2} = 2800$ m/s.

It is also important to notice that the PS-wave reflection coefficient has a peak corresponding to the critical PP reflection (Mehdizadeh et al., 2005). Therefore, PS-wave amplitude analysis can help to get a more reliable estimate of the critical angle of PP-waves.

WHAT CAN BE DETERMINED FROM THE CRITICAL ANGLE?

The analytic results in the previous section indicate that measurements of the critical angle contain valuable information for anisotropic parameter estimation. Here, we explore the parameter-estimation issues in more detail for both VTI and orthorhombic models.

VTI media

If the vertical-velocity ratio n has been determined, for example, from borehole data, an estimate of the P-wave critical angle can be used to constrain the parameters ϵ and δ . For a VTI layer beneath an isotropic overburden, the angle θ_{cr} depends just on ϵ_2 , the parameter responsible for the horizontal velocity in the reflecting medium (equations 1 and 3):

$$\epsilon_2 = \frac{1}{2} \left(\frac{n^2}{\sin^2 \theta_{cr}} - 1 \right). \quad (20)$$

In the weak-anisotropy approximation, ϵ_2 can be found from equation 9:

$$\epsilon_2 = 1 - \frac{\sin \theta_{cr}}{n}. \quad (21)$$

When the reflecting medium is isotropic, while the overburden is VTI, there are two unknowns (ϵ_1 and δ_1) in equation 9, and this ambiguity cannot be resolved without additional information. For the general VTI/VTI model, measurement of the critical angle provides a relationship between the parameters ϵ_1 , δ_1 , and ϵ_2 . Since equation 9

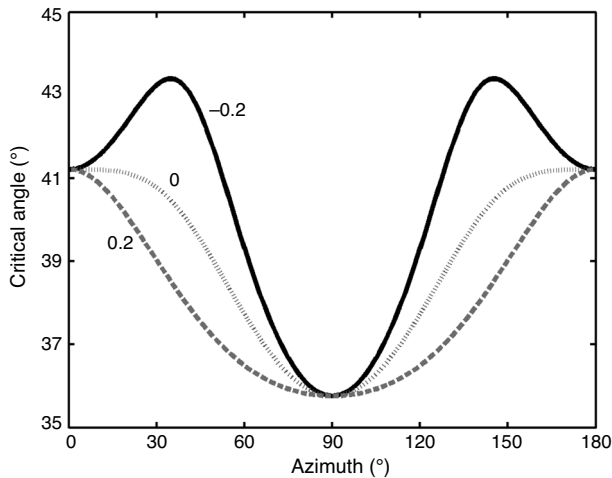


Figure 7. Influence of the parameter $\delta_2^{(3)}$ on the exact P-wave critical angle for an interface between isotropic (incidence) and orthorhombic (reflecting) media. The curves are computed for $\delta_2^{(3)}$ equal to -0.2 (solid), 0 (dotted), and 0.2 (dashed). The other relevant parameters of the orthorhombic medium are $V_{p0,2} = 2800$ m/s, $\epsilon_2^{(2)} = 0.25$, and $\epsilon_2^{(1)} = 0.1$. The P-wave velocity in the isotropic medium is $V_{p0,1} = 2100$ m/s.

represents a linearized approximation, more accurate estimates of the anisotropy parameters can be obtained by solving equation 1 with the exact velocity function.

Orthorhombic media

In the azimuthal AVO analysis, the best-constrained parameter is the difference between the AVO gradients in the vertical symmetry planes (e.g., Rüger, 2001). Likewise, the critical-angle reflectometry can provide an estimate of the difference $\Delta(\sin \theta_{cr})$ between the symmetry-plane critical angles. As follows from equation 15,

$$\begin{aligned} \Delta(\sin \theta_{cr}) &\equiv \sin \theta_{cr}(0^\circ) - \sin \theta_{cr}(90^\circ) \\ &= -(\Delta\epsilon_2)n + (\Delta\delta_1)n^3 + (\Delta\epsilon_1 - \Delta\delta_1)n^5, \end{aligned} \quad (22)$$

where $\Delta\delta_1 = \delta_1^{(2)} - \delta_1^{(1)}$, $\Delta\epsilon_1 = \epsilon_1^{(2)} - \epsilon_1^{(1)}$, and $\Delta\epsilon_2 = \epsilon_2^{(2)} - \epsilon_2^{(1)}$. When both media are orthorhombic, equation 22 contains three independent anisotropic parameter combinations, which cannot be resolved without additional constraints.

However, for the simplest case of a purely isotropic overburden, the only anisotropy parameter that influences the critical angle is $\epsilon_2(\phi)$. Then $\Delta(\sin \theta_{cr})$ can be used to find the difference between $\epsilon_2^{(2)}$ and $\epsilon_2^{(1)}$:

$$\Delta\epsilon_2 = -\frac{\Delta(\sin \theta_{cr})}{n}. \quad (23)$$

If reliable measurements of $\sin \theta_{cr}$ in both symmetry planes are available, the parameters $\epsilon_2^{(1)}$ and $\epsilon_2^{(2)}$ can be resolved individually using the VTI equation 20.

As discussed, the azimuthally varying critical angle may have maxima or minima between the symmetry planes. The azimuth and magnitude of these extrema are quite sensitive to the parameter $\delta_2^{(3)}$ of the reflecting medium, which influences the horizontal velocity outside the symmetry planes (Figure 7). Therefore, if the incidence medium is isotropic (or if its parameters are known) and the data have dense azimuthal coverage, the function $\sin \theta_{cr}(\phi)$ can be inverted for all three relevant anisotropy parameters of the reflecting medium ($\epsilon_2^{(1)}$, $\epsilon_2^{(2)}$, and $\delta_2^{(3)}$).

ESTIMATION OF THE CRITICAL ANGLE FROM REFLECTION DATA

To identify the critical angle on surface reflection data, it is necessary to analyze the amplitude of the reflected wave at near-critical offsets. We start by computing the reflection coefficient of plane P-waves for an interface between isotropic and orthorhombic media and then generate complete synthetic seismograms that include both the reflected and head waves.

Near-critical reflection amplitude

The behavior of the reflection coefficient near the critical angle is seldom analyzed in exploration seismology because conventional processing techniques operate with subcritical reflection data. It is well known from both analytic and numerical results for isotropic media that the reflection coefficient rapidly increases toward the critical angle, where its derivative becomes infinite (Aki and Richards, 2002; Tsvankin, 1995). The P-wave reflection coefficient for an in-

terface between isotropic and orthorhombic media in Figure 8 varies with azimuth, but its shape near the azimuthally dependent critical angle $\theta_{cr}(\phi)$ is practically the same. After a sharp peak at θ_{cr} , the real part of the reflection coefficient slowly decreases in the post-critical domain. (Note that the critical angles for all four azimuths are in excellent agreement with our computations for this model in Figure 4.)

The AVO curve of the reflected wave at near-critical incidence, however, is not determined exclusively by the plane-wave reflection coefficient. First, because the amplitude of the reflected wave (as opposed to the reflection coefficient) has a continuous derivative, it increases beyond θ_{cr} . Second, the reflected wave in the post-critical domain undergoes rapid phase changes and interferes with the head wave. For a range of post-critical offsets, the reflected and head waves form a single arrival that cannot be described by the geometric-seismics approximation based on the plane-wave reflection coefficient (Červený, 1962; Tsvankin, 1995).

With the increased separation between the two waves, their interference (tuning) produces a frequency-dependent AVO curve that does not follow the angle dependence of the plane-wave reflection coefficient. In particular, the amplitude maximum of this interference arrival is shifted toward *post-critical* offsets, while the critical angle is generally close to the point of the fastest amplitude increase (Červený, 1961, 1962). Although Červený's analysis is limited to isotropic models, this conclusion agrees with our exact modeling results for an isotropic/orthorhombic interface. It should be emphasized, however, that the shift of the amplitude maximum with respect to the critical offset x_{cr} varies with frequency and the model parameters.

Synthetic example using reflectivity modeling

To test the proposed method on synthetic reflection data, we computed the wavefield for a simple model that includes an orthorhombic layer beneath an isotropic medium (Figure 9). The seismograms were generated with the anisotropic reflectivity method (Chin et al.,

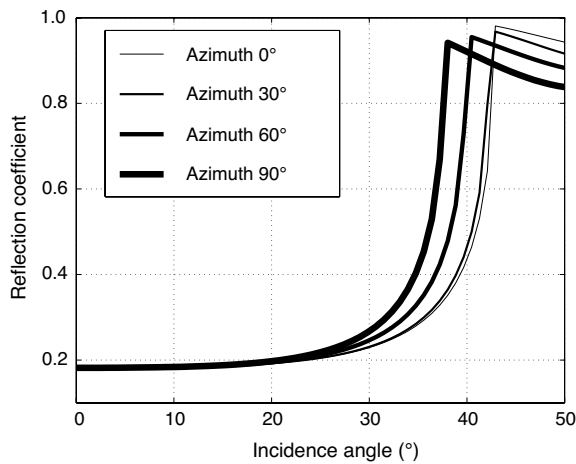


Figure 8. Real part of the exact P-wave reflection coefficient computed in four azimuthal directions for an interface between isotropic (incidence) and orthorhombic (reflecting) media. The velocities in the incidence medium are $V_{p0,1} = 2100$ m/s and $V_{s0,1} = 1200$ m/s, the density $\rho_1 = 2.4$ g/cm³. For the reflecting medium, $V_{p0,2} = 2800$ m/s, $V_{s0,2} = 1200$ m/s, $\rho_2 = 2.6$ g/cm³, $\epsilon_2^{(1)} = 0.25$, $\epsilon_2^{(2)} = 0.1$, $\delta_2^{(1)} = 0.05$, $\delta_2^{(2)} = -0.1$, $\delta_2^{(3)} = -0.1$, $\gamma_2^{(1)} = 0.28$, and $\gamma_2^{(2)} = 0.15$. The azimuthally varying critical angle for this model is plotted in Figure 4.

1984), which produces exact 3D wavefields for horizontally layered media. Our goal was to estimate the critical angle for the PP-wave reflection from the top of the orthorhombic layer (see the arrows).

Figure 9 shows long-spread synthetic gathers computed in the vertical symmetry planes of the model. For both azimuths, there is a weak, but clearly visible head wave splitting off from the PP-wave reflection. The separation of the head wave occurs at a smaller offset for the azimuth $\phi = 90^\circ$, which is indicative of a decrease in the critical angle. As explained previously, we associate the critical offset with the point of the fastest amplitude increase (i.e., the inflection point corresponding to the largest slope) on the AVO curves (Figure 10). The angle θ_{cr} , which was computed from the critical offset using the known velocity in the incidence medium, is close to 43° for $\phi = 0^\circ$ and 38.5° for $\phi = 90^\circ$.

The estimated critical angle in Figure 11 is close to the exact value for the full range of azimuths. If the vertical/velocity ratio is known, our measurements of θ_{cr} can be inverted for all three relevant parameters of the orthorhombic medium: $\epsilon_2^{(1)}$, $\epsilon_2^{(2)}$, and $\delta_2^{(3)}$ (Figure 7). Note that the linearized approximation 23 for this model gives an error in $\epsilon_2^{(1)} - \epsilon_2^{(2)}$ of about 0.05.

The anisotropy parameters in the reflecting layer can also be estimated from the head-wave velocity. For laterally homogeneous media, the slope (dx/dt) of the linear moveout of the head wave is equal to the horizontal velocity $V_{hor,2}$ in the reflecting medium. Measurements of the velocity $V_{hor,2}$ for a wide range of source-receiver azimuths can be inverted for the parameters $\epsilon_2^{(1)}$, $\epsilon_2^{(2)}$, and $\delta_2^{(3)}$. We used the synthetic seismograms for the model in Figure 9 to estimate the slope of the head-wave moveout and then substituted the values of $V_{hor,2}$ into equation 1 to compute the critical angle. The obtained function $\theta_{cr}(\phi)$ in Figure 12 is even more accurate than that estimated from the AVO curve, which confirms the feasibility of using the moveout of head waves in parameter estimation. (The velocity $V_{hor,2}$ can be inverted directly for the anisotropy parameters of the reflecting layer without computing the critical angle.) In practice, however,

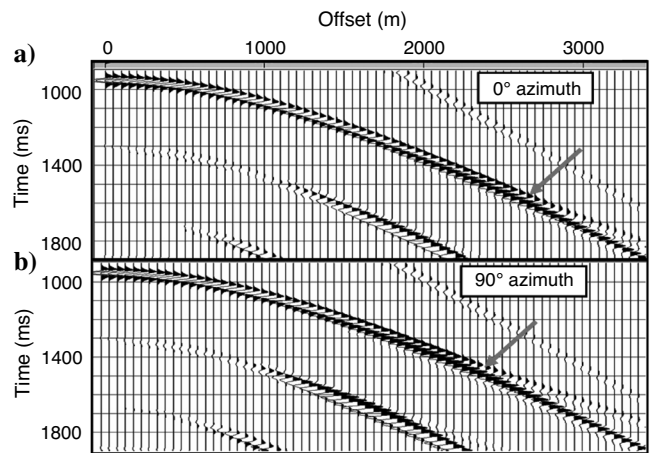


Figure 9. Synthetic shot gathers of the vertical displacement for the wavefield reflected from an orthorhombic layer. The sources and receivers are located in an isotropic half-space (the free surface is removed); the model parameters are the same as in Figure 8. The traces are plotted for a wide range of offsets in the vertical symmetry planes: (a) $\phi = 0^\circ$ and (b) $\phi = 90^\circ$. The zero-offset traveltime for the PP-wave reflection from the top of the orthorhombic layer is about 950 ms. Notice the head wave splitting off from the reflected wave at offsets (marked by the arrows) between 2000 and 3000 m.

it may be difficult to operate with head waves because their amplitudes are relatively small and the long offsets required for their detection are seldom available.

DISCUSSION

Implementation of critical-angle reflectometry requires considering several important practical issues. First, the critical-angle reflection can be recorded only if there is a significant velocity increase at the top or bottom of the reservoir. (Most carbonate and consolidated sand reservoirs have a higher velocity than that in the overburden.) Second, the method has to operate on wide-azimuth, long-offset data that include the critical reflected ray from the target interface. Third, the critical-angle reflection may be obscured by the overburden noise train, which can be partially attenuated by f - k filtering and similar processing techniques. We expect that a more efficient removal of overburden noise can be achieved by model-based inversion. Also, despite the generally high level of noise at far offsets, the sharp

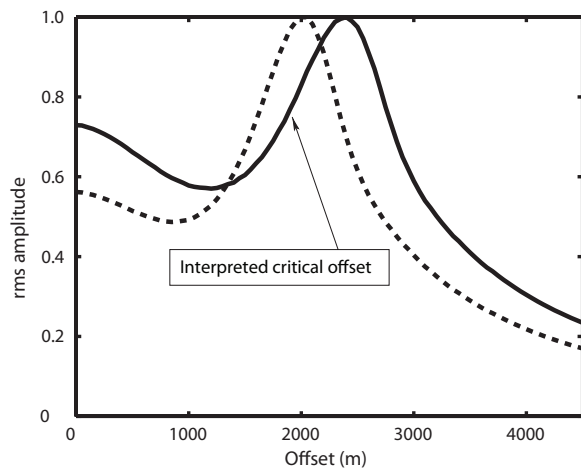


Figure 10. Amplitude of the reflected PP-wave from Figure 9 as a function of offset for the azimuths $\phi = 0^\circ$ (solid curve) and $\phi = 90^\circ$ (dashed). The arrow marks the point of the fastest amplitude increase (i.e., of the largest slope of the AVO curve) for $\phi = 0^\circ$.

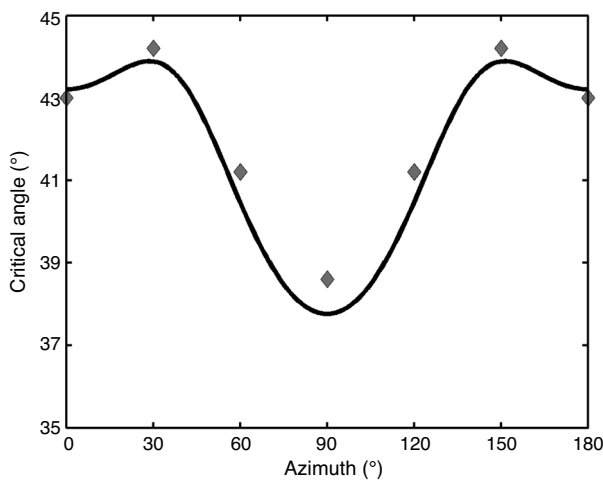


Figure 11. Variation of the critical angle with azimuth for the model from Figure 9. The diamonds mark θ_{cr} estimated from the reflectivity modeling. The solid line is the exact value.

amplitude increase near the critical angle should help in detecting the critical offset.

Quantitative analysis of critical-angle measurements faces a number of serious challenges. One of them is related to the estimation of the critical offset x_{cr} from AVO curves. The synthetic test discussed above shows that the point of the fastest amplitude increase (the inflection point) does not exactly correspond to x_{cr} . In general, the shift of the critical offset with respect to the amplitude maximum is frequency-dependent. Therefore, it is desirable to verify the obtained value of x_{cr} by computing the AVO curve using the velocity model built after application of critical-angle reflectometry (possibly in combination with other methods). Also, instead of using the inflection point, it may be possible to estimate the critical angle by picking the offset of the amplitude maximum and applying a model-dependent offset shift.

If the overburden is anisotropic, the AVO response of reflected waves can be distorted by angle-dependent geometric spreading. However, in the absence of strong heterogeneity in the overburden, geometric spreading of P-waves varies slowly with offset and is unlikely to have a major impact in the narrow range of near-critical offsets used in our method. Also, note that the anisotropic geometric-spreading factor can be computed directly from reflection travel-times and removed from the AVO response (Xu and Tsvankin, 2006; also see Xu et al., 2005). Although the method of Xu and Tsvankin (2006) is designed for laterally homogeneous models, it remains sufficiently accurate in the presence of moderate lateral velocity variations and mild interface dips of up to 15° .

Even if the critical offset has been accurately estimated from the reflection amplitude, computation of the corresponding critical angle at the target horizon requires knowledge of the overburden velocity model. An apparent variation of the critical offset can be created by reflector dip, although for mild dips of several degrees such offset distortions are insignificant. For anisotropic media it is also necessary to account for the difference between the group (ray) angle responsible for the critical offset and the phase angle of the critical ray that was analyzed in our paper. While conventional AVO analysis has to deal with the same problem, our method is more sensitive to errors in the offset-to-angle conversion because it relies on a single angle measurement for a given azimuth.

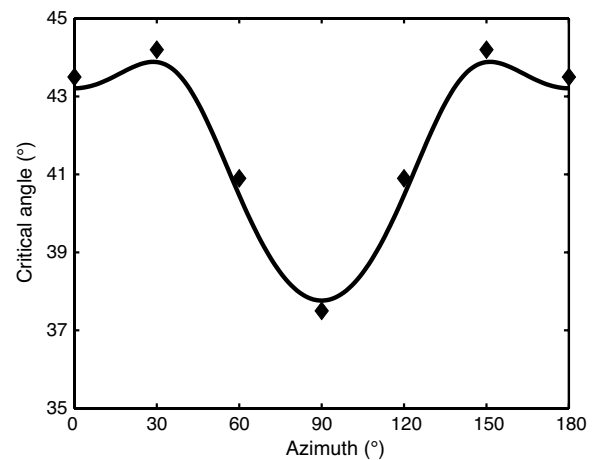


Figure 12. Same as Figure 11, but the diamonds mark the critical angle estimated from the horizontal velocity of the head wave.

The transition from the critical offset to the critical angle may be avoided for models with a laterally homogeneous overburden. The amplitude of the reflected wave can be treated as a function of the ray parameter (horizontal slowness), which is estimated from the slope of the moveout curve. In the absence of lateral heterogeneity, the ray parameter at the critical offset is equal to the horizontal slowness in the high-velocity layer. Therefore, the moveout slope of the critical-angle event gives a direct estimate of the horizontal velocity in the reflecting layer. For data sets with uncommonly long offsets, the horizontal velocity can also be determined from the linear moveout of the head wave (Figure 12). Note that for laterally homogeneous models, it may be advantageous to identify the critical-angle reflection by applying the τ - p transform (Van der Baan, 2005).

The azimuthally varying horizontal velocity in the reflecting orthorhombic layer can be inverted for the difference $\epsilon^{(1)} - \epsilon^{(2)}$ and for the parameter $\delta^{(3)}$ without knowledge of the overburden velocity model. Furthermore, the horizontal velocities in the vertical symmetry planes can be combined with the symmetry-plane NMO velocities to compute the anellipticity parameters $\eta^{(1)}$ and $\eta^{(2)}$ responsible for time processing of P-wave data (Grechka and Tsvankin, 1999). If the reflecting layer has VTI symmetry, the combination of the horizontal and NMO velocities yields the parameter η , which controls anisotropic P-wave time imaging.

CONCLUSIONS

We introduced a method that can be called *seismic critical-angle reflectometry* because it is based on measuring the critical angle θ_{cr} on reflection seismic data. When the medium above or below the reflector is anisotropic, the angle θ_{cr} is strongly influenced by the anisotropy parameters. In particular, the azimuthal variation of the critical angle estimated from wide-azimuth surveys can provide sensitive attributes for fracture characterization.

Using the weak-anisotropy approximation, we obtained concise expressions for the critical angles of pure and mode-converted waves in VTI and orthorhombic media. For vertical transverse isotropy, the P-wave angle θ_{cr} is particularly sensitive to the Thomsen parameter ϵ of the reflecting medium and also depends on the parameters ϵ and δ of the incidence medium. With the azimuthally varying parameters ϵ and δ , the VTI equation for the critical angle remains valid for wide-azimuth, P-wave data from orthorhombic media.

For a VTI layer beneath an isotropic overburden, the angle θ_{cr} can be inverted for the parameter ϵ , which is difficult to obtain from conventional-spread reflection data. When the reflecting layer is orthorhombic, the azimuthally dependent critical angle can be used to estimate the anisotropy parameters $\epsilon^{(1)}$, $\epsilon^{(2)}$, and $\delta^{(3)}$ responsible for the P-wave horizontal velocity. The azimuthal variation of θ_{cr} also helps to identify the symmetry-plane directions, which often coincide with the dominant fracture azimuths.

If the medium is laterally homogeneous, the ray parameter of the critical-angle reflection is equal to the inverse of the horizontal velocity in the high-velocity layer. The azimuthal variation of the horizontal velocity in orthorhombic media can be used to estimate the difference $\epsilon^{(1)} - \epsilon^{(2)}$ and the parameter $\delta^{(3)}$ without knowledge of the overburden velocity model. Also, by combining the symmetry-plane horizontal and NMO velocities, one can obtain the time-processing parameters $\eta^{(1)}$ and $\eta^{(2)}$.

We verified the analytic results for the isotropic/orthorhombic interface by computing synthetic seismograms with the reflectivity method and estimating the critical angle from the point of the fastest

amplitude increase on the AVO curve of the reflected wave. Although this point tends to be slightly shifted from the critical ray toward larger offsets, the computed critical angle is close to the exact value. The synthetic test also confirms that the extrema of the azimuthally varying function θ_{cr} do not necessarily correspond to the symmetry planes, which underscores the need for dense azimuthal coverage in critical-angle reflectometry.

On the whole, we do not envision critical-angle reflectometry as a reliable stand-alone method for anisotropic parameter estimation. Rather, it should be used in combination with existing anisotropic inversion techniques that operate with azimuthally varying travel-times and amplitudes.

ACKNOWLEDGMENTS

We are grateful to our colleagues at the Center for Wave Phenomena (CWP), Colorado School of Mines (CSM), for useful discussions, to Xiaoxia Xu (CSM) for her help with the reflectivity modeling and numerous suggestions, and to Barbara McLenon (CSM) for technical assistance. We thank the Grane Partnership (Hydro, Petro, ExxonMobil, and ConocoPhillips) for providing data from the Grane Field and permission to publish our results. Jan Petter Fjellanger, Ivar Sandø, and Frede Bøen (all of Hydro) are acknowledged for support and discussions. The suggestions of the editors and reviewers of *GEOPHYSICS* (in particular, Vladimir Grechka and Mirko van der Baan) helped to improve the paper. The anisotropic modeling software was developed by Dennis Corrigan (formerly of ARCO). Martin Landrø acknowledges CSM and CWP for their hospitality during his sabbatical visit and the Norwegian Research Council for financial support of the ROSE (Rock Seismic) project at NTNU. This work was partially supported by the Consortium Project on Seismic Inverse Methods for Complex Structures at CWP.

REFERENCES

- Aki, K., and P. G. Richards, 2002, *Quantitative seismology*: University Science Books.
- Alkhalifah, T., 1997, Velocity analysis using nonhyperbolic moveout in transversely isotropic media: *Geophysics*, **62**, 1839–1854.
- Alkhalifah, T., and I. Tsvankin, 1995, Velocity analysis for transversely isotropic media: *Geophysics*, **60**, 1550–1566.
- Antich, P., and S. Mehta, 1997, Ultrasound critical-angle reflectometry (UCR): A new modality for functional elastometric imaging: *Physics in Medicine and Biology*, **42**, 1763–1777.
- Bakulin, A., V. Grechka, and I. Tsvankin, 2000, Estimation of fracture parameters from reflection seismic data — Part II: Fractured models with orthorhombic symmetry: *Geophysics*, **65**, 1803–1817.
- Červený, V., 1961, The amplitude curves of reflected harmonic waves around the critical point: *Studia Geophysica et Geodaetica*, **5**, 319–351.
- Červený, V., 1962, On the position of the maximum of the amplitude curves of reflected waves: *Studia Geophysica et Geodaetica*, **6**, 215–233.
- Chin, R., G. W. Hedstrom, and L. Thigpen, 1984, Matrix methods in synthetic seismograms: *Geophysical Journal of the Royal Astronomical Society*, **77**, 483–502.
- Gray, F. D., G. Roberts, and K. J. Head, 2002, Recent advances in determination of fracture strike and crack density from P-wave seismic data: *The Leading Edge*, **21**, 280–285.
- Grechka, V., and M. Kachanov, 2006, Seismic characterization of multiple fracture sets: Does orthotropy suffice?: *Geophysics*, **71**, no. 3, D93–D105.
- Grechka, V., A. Pech, and I. Tsvankin, 2005, Parameter estimation in orthorhombic media using multicomponent wide-azimuth reflection data: *Geophysics*, **70**, no. 2, D1–D8.
- Grechka, V., and I. Tsvankin, 1998, Feasibility of nonhyperbolic moveout inversion in transversely isotropic media: *Geophysics*, **63**, 957–969.
- , 1999, 3-D moveout velocity analysis and parameter estimation for orthorhombic media: *Geophysics*, **64**, 820–837.
- Hall, S., and J. M. Kendall, 2003, *Fracture characterization at Valhall*: Appli-

- cation of P-wave amplitude variation with offset and azimuth (AVOA) analysis to a 3-D ocean-bottom data set: *Geophysics*, **68**, 1150–1160.
- Helbig, K., 1994. *Foundations of elastic anisotropy for exploration seismics*: Pergamon Press, Inc.
- Jilek, P., 2002, Modeling and inversion of converted-wave reflection coefficients in anisotropic media: A tool for quantitative AVO analysis: Ph.D. dissertation, Colorado School of Mines.
- Landrø, M., A. K. Nguyen, and H. Mehdizadeh, 2004, Time lapse refraction seismic — A tool for monitoring carbonate fields?: 74th Annual International Meeting, SEG, Expanded Abstracts, 2295–2298.
- Mehdizadeh, H., M. Landrø, B. A. Mythen, N. Vedanti, and R. Srivastava, 2005, Time lapse seismic analysis using long-offset PS data: 75th Annual International Meeting, SEG, Expanded Abstracts, TL 3.7.
- Pankhurst, D., K. Marfurt, C. Sullivan, H. Zhou, F. Hilterman, and J. Gallagher, 2002, Long offset AVO in a mid-continent tight gas sand reservoir: 72nd Annual International Meeting, SEG, Expanded Abstracts, 297–299.
- Pech, A., and I. Tsvankin, 2004, Quartic moveout coefficient for a dipping azimuthally anisotropic layer: *Geophysics*, **69**, 699–707.
- Rüger, A., 2001, Reflection coefficients and azimuthal AVO analysis in anisotropic media: SEG.
- Thomsen, L., 1986, Weak elastic anisotropy: *Geophysics*, **51**, 1954–1966.
- Toldi, J., T. Alkhalifah, P. Berthet, J. Arnaud, P. Williamson, and B. Conche, 1999, Case study of estimation of anisotropy: *The Leading Edge*, **18**, 588–594.
- Tsvankin, I., 1995, *Seismic wavefields in layered isotropic media*: Samizdat Press.
- , 1997, Anisotropic parameters and P-wave velocity for orthorhombic media: *Geophysics*, **62**, 1292–1309.
- , 2005, *Seismic signatures and analysis of reflection data in anisotropic media*, 2nd ed.: Elsevier Science Publishing Co., Inc.
- Tsvankin, I., and V. Grechka, 2006, Developments in seismic anisotropy: Treating realistic subsurface models in imaging and fracture detection: *Canadian Society of Exploration Geophysicists Recorder*, **31**, 43–46.
- Van der Baan, M., 2005, Processing of anisotropic data in the τ - p domain: II — Common-conversion-point sorting: *Geophysics*, **70**, no. 4, D29–D36.
- Vasconcelos, I., and I. Tsvankin, 2006, Nonhyperbolic moveout inversion of wide-azimuth P-wave data for orthorhombic media: *Geophysical Prospecting*, **54**, 535–552.
- Xu, X., and I. Tsvankin, 2006, Anisotropic geometrical-spreading correction for wide-azimuth P-wave reflections: *Geophysics*, **71**, no. 5, D161–D170.
- Xu, X., I. Tsvankin, and A. Pech, 2005, Geometrical spreading of P-waves in horizontally layered, azimuthally anisotropic media: *Geophysics*, **70**, no. 5, D43–D54.